

## Real-time magnetic equilibria for NTM stabilisation experiments

L.Giannone, M.Reich, W.Treutterer, R.Fischer, J.C.Fuchs, K.Lackner,  
M.Maraschek, P.J.McCarthy<sup>1</sup>, R.Preuss, M.Rampp and the ASDEX Upgrade Team

*Max-Planck-Institut für Plasmaphysik,*

*EURATOM-IPP Association, D-85748 Garching, Germany*

<sup>1</sup>*Department of Physics, University College Cork, Association EURATOM-DCU, Cork, Ireland*

### Introduction

Real-time magnetic equilibria in ASDEX Upgrade are required for the microwave beam tracing code, TORBEAM [1], to calculate the mirror angle necessary for depositing ECCD current on the rational surface where a neoclassically driven tearing mode island, NTM, is located. This scheme for suppression of NTM's seeks to improve tokamak performance by raising the operational limits on poloidal beta,  $\beta_p$  [2, 3].

### Vacuum field calibration

A detailed optimization process is carried out once a year to ensure that the assumed geometry and orientation of the magnetic probes, the position of the poloidal field coils, the calibration factors of the poloidal field currents and the calibration factors of magnetic probe and flux loop integrators are self consistent. The minimization of the least squares difference of the predicted and measured signals is found using a steepest descent algorithm. A self consistent set of calibration factors for calculating magnetic equilibria is the result.

The first step of the optimization process is concerned solely with finding the set of gains of the integrators of the magnetic probes and Rogowski coils to minimize the root mean square error of the difference between the predicted value and measured value of magnetic probes and flux loops in response to the excitation of each of the 11 poloidal field coils. The nominal position of the poloidal field coils and the variation in position and angle of the magnetic probes are also possible variables for optimization. In the second step, a steepest descent algorithm is used to optimize the positions of the flux loops. A factor of 4 reduction in the mean square error could be achieved. Allowing variations in the poloidal field coil positions reduced the root mean square error by a further 10%. Position shifts of the order up to 2 centimeters in the radial and vertical direction were required to achieve this fit. In the final stage the radial position, vertical position and angle of the 40 magnetic probes were allowed to vary and this led to a further reduction in the root mean square error of 20%. In the final analysis with 600 iterations of the optimization algorithm, a root mean square error of 0.7 mT could be achieved for the difference between the measured and predicted values.

### Real-time Grad-Shafranov solver

A real-time Grad-Shafranov solver based on the rtEFIT algorithm [4], constrained to fit 40 magnetic probes and 18 flux loop differences, is used to calculate the magnetic equilibrium. An innovative algorithm, using discrete sine transforms and a tridiagonal solver, realises an equilibrium poloidal flux matrix for 4 basis current functions on a 33x65 grid in 0.49 ms on a dual quad core Xeon 5677 computer with LabVIEW RT 2011 [5, 6]. The real-time application with data acquisition and real-time communication presently runs with a 4.5 ms cycle time. A dual octal core Xeon E5-2687 computer is planned and a reduction in cycle time by about a factor of 2 is expected.

Real-time communication is carried out with a x4 PCIe VMIC 5565 PIORC reflective memory card. The reflective memory card transmits the 33x65 poloidal flux matrix values to the control system with less than 1 ms delay. For diagnostics not connected to the reflective memory network, a compressed flux matrix that fits into a UDP packet is available. The compression performs a two dimensional discrete cosine transform (DCT) and sends the 253 DCT coefficients for reconstruction of the poloidal flux matrix to the remote real-time diagnostic.

An  $m/n=3/2$  NTM mode was present in a 1 MA discharge with 10 MW NBI heating and 2MW ECRH heating. The time evolution of the radial location of 3 rational  $q$  surfaces is shown in Figure 1. The location of the  $m/n=3/2$  NTM can also be inferred from temperature fluctuation measurements at the mode frequency of the NTM. The phase jump of the fluctuation is related to the change in phase of the temperature fluctuation around the NTM magnetic island. These measurements indicate that the NTM is located at a normalised radius of about 0.4 [3]. It is possible to choose basis current profiles for the Grad-Shafranov solver, so that the predicted normalised radius is sufficiently accurate to perform NTM stabilisation experiments for experiments where MSE measurements are not available. The ability to move the predicted radial position of the rational  $q$  surface with appropriate choice of current basis functions is demonstrated in Fig. 2. The central current basis profile is less peaked in this case.

### MSE constraints

The real-time Grad-Shafranov solver has been extended to include constraints on the current profile in the plasma core from the Motional Stark Effect, MSE, diagnostic. A second Grad-Shafranov solver that also fits ten spatially localized measurements from the Motional Stark effect diagnostic [7], runs in parallel to the solver constrained by magnetic measurements only. The accuracy of the  $q$  profile is improved by the measurements of the polarization angle,  $\gamma_m$  :

$$\tan(\gamma_m) = \frac{c1 * B_r + c2 * B_t + c3 * B_z + c4 * E_r / v_{Beam}}{c5 * B_r + c6 * B_t + c7 * B_z + c8 * E_r / v_{Beam} + c9 * E_z / v_{Beam}} \quad (1)$$

where  $c1..c9$  are a set of coefficients for each channel relating the local components of electric field ( $E_r$  and  $E_z$ ), magnetic field ( $B_r$  and  $B_z$ ) and diagnostic beam velocity,  $v_{beam}$ , to  $\gamma_m$  [8]. The components of the poloidal magnetic field at the centre of the measurement volume are evaluated by a matrix-vector multiplication using pre-calculated Green's functions. The toroidal component of the magnetic field,  $B_t$ , is calculated from :

$$(RB_t)^2 = (R_o B_o)^2 + 2 \int_{\Psi_{boundary}}^{\Psi} FF' d\Psi \quad (2)$$

where  $FF'$  are those terms of the current profile representing the poloidal current. The integrals of the current basis functions are tabulated. Neglecting terms in  $E_r$  and  $E_z$  in Equation 1, the expression for the response matrix for each MSE channel becomes :

$$(c1 - c5 * \tan(\gamma_m)) * (B_{rp} + B_{rc}) + (c3 - c7 * \tan(\gamma_m)) * (B_{zp} + B_{zc}) = -(c2 - c6 * \tan(\gamma_m)) B_t \quad (3)$$

The left hand side terms of the response matrix are the magnetic field components,  $B_{rp}$  and  $B_{zp}$  calculated for each MSE measurement volume and for each current basis function. The  $B_{rc}$  and  $B_{zc}$  are the components due to currents in the the poloidal field coils for each MSE measurement volume and are transferred to the right hand side of the above equation. The ten additional constraints on the response matrix typically allows the number of fit coefficients to be raised from 4 to 6 [7]. It is known that neglecting the terms in electric field leads to differences in the central safety factor,  $q_o$  [9].

A simulation of the MSE diagnostic measurements was performed to test the application. The expected  $\tan(\gamma_m)$  for an equilibrium fitting the magnetic probes and flux loops was calculated and subsequently used to calculate an equilibrium using magnetics and the simulated MSE measurements. In Figures 3 and 4 the simulated and fitted terms of Equation 3 used in the Grad-Shafranov solver for each MSE measurement volume are plotted. The predicted location of the  $m/n$  rational surfaces when using the MSE constraints with 6 basis current functions reproduces the predicted location when using magnetics alone to constrain the Grad-Shafranov solver.

## Conclusion

A real-time Grad Shafranov solver including MSE constraints is being commissioned for NTM stabilization experiments on ASDEX Upgrade. The offline version, without data acquisition and real-time communication, achieves a cycle time of 0.8 ms for 6 basis current functions on a 33 by 65 grid. The application with data acquisition and real-time communication is being brought into operation and a cycle time of less than 3 ms is expected.

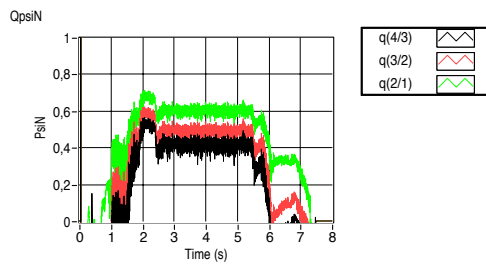


Figure 1: Time traces of the normalized radius of the rational  $q$  surface with a centrally peaked current basis function and the  $m/n=3/2$  surface at  $\rho = 0.45$ .

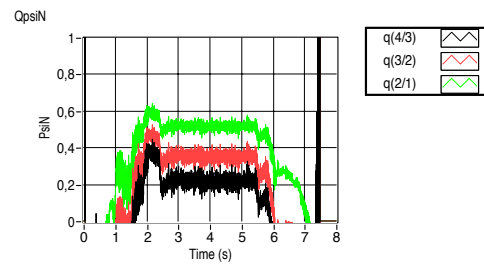


Figure 2: Time traces of the normalized radius of the rational  $q$  surface with the basis current function tuned to place the  $m/n=3/2$  surface at  $\rho = 0.35$ .

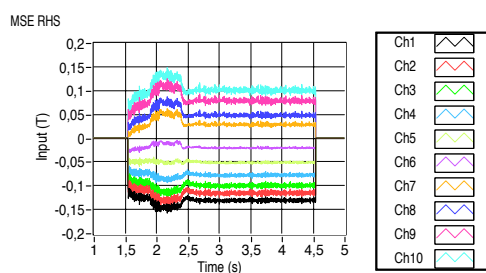


Figure 3: Time traces of the simulated right hand side of Equation 3 for each MSE measurement.

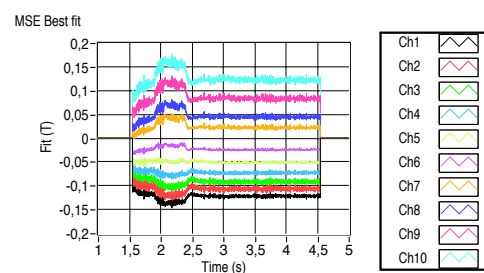


Figure 4: Time traces of the fitted right hand side of Equation 3 for each MSE measurement.

## References

- [1] E. Poli et al., *Comp. Phys. Comm.* **136**, 90 (2001)
- [2] M.Maraschek et. al, *Nucl. Fusion* **45**, 1369 (2005)
- [3] M.Reich et al., Progress on ECCD-based NTM rt-control at ASDEX Upgrade, EPS 2011
- [4] J.R.Ferron, M.L.Walker, L.L.Lao et. al, *Nucl. Fusion*, **38**, 1055 (1998)
- [5] L.Giannone et. al, <http://accelconf.web.cern.ch/AccelConf/pcapac2010/papers/thpl024.pdf>
- [6] R. Preuss, R. Fischer, M. Rampp, K. Hallatschek, U. von Toussaint, L. Giannone, P. McCarthy, IPP-Report R/47 (2012)
- [7] L. L. Lao, H. E. St. John, Q. Peng et. al, *Fusion Science and Technology*, **48**, 968 (2005)
- [8] D.Wroblewski and L.L.Lao, *Rev. Sci. Instrum.* **63**, 5140 (1992)
- [9] B.W.Rice, D.G.Nilson, K.H.Burrell, and L.L.Lao, *Rev. Sci. Instrum.*, **70**, 815 (1999)